GROUND MOTION CHARACTERISTICS IN THE GRABEN-LIKE IRREGULAR UNDERGROUND STRUCTURE FOR FINITE MOVING SOURCE WITH DIFFERENT SLIP SIZE

Masato MOTOSAKA[1] And Ali NIOUSHA[2]

SUMMARY

Theoretical ground motion characteristics taking into account the variable slip source and the deep irregular underground structure are analytically investigated using hyperelement method. The 3D wave propagation analyses have been performed using the 2D graben-like irregular underground structure model of Kobe City. The ground motion characteristics are discussed for different asperity sizes. Ground motion amplification characteristics at sediment site to rock site are discussed for one-asperity models with different size and also for two asperities models. Three components, fault normal (FN), fault parallel (FP) and vertical (UD), of velocity waveforms and distributions of PGVs are investigated for different wavefields. The following findings are obtained. The amplitudes of the calculated ground motions in the FN direction are larger than the FP direction as recognized in the observed near-source ground motions. The FN/FP ratio becomes larger as slip size becomes smaller. The PGVs in the FN direction become large in the same range corresponding to the heavily damaged area. The vertical PGVs become large at the sediment site in the vicinity of the rock-sediment boundary. These results are the same as those for plane incident waves, deconvoluted from the observation records at Kobe University. The PGVs are larger in the small asperity case compared to the large asperity case when the total seismic moments are the same. The higher frequency contents are generated at the rock site and the higher resonant frequencies are stimulated at the sediment site, as the slip size becomes smaller. The calculated waveforms show strong forward directivity in the propagation direction due to a finite moving source. The shape of the PGV distribution for one asperity can be changed due to the interference of the wavefields for two asperities when they are closed.

INTRODUCTION

It is important to investigate the near-source ground motion characteristics in seismic design of building structures and in urban disaster prevention for the near-source earthquake. It has been reported that the graben-like irregular underground structure caused the heavily damaged belt zone during the 1995 Hyogo-ken Nanbu earthquake [Motosaka and Nagano, 1997]. Theoretical ground motion characteristics taking into account variable slip sources and the deep irregular underground structure for one asperity cases were investigated. Particularly, horizontal ground motion characteristics focused on the dominant period contents, distribution of the peak values and directionality of ground motion were discussed for different slip distributions on fault plane [Motosaka and Takenaka, 1998]. In this paper, the authors discuss the horizontal as well as the vertical ground motion characteristics for one and two asperities cases.

[1] *Disaster Control Research Center, Tohoku University, JAPAN motosaka@struct.archi.tohoku.ac.jp*
[2] *Disaster Control Research Center, Graduate School of Engineering, Tohoku University, Sendai - JAPAN*

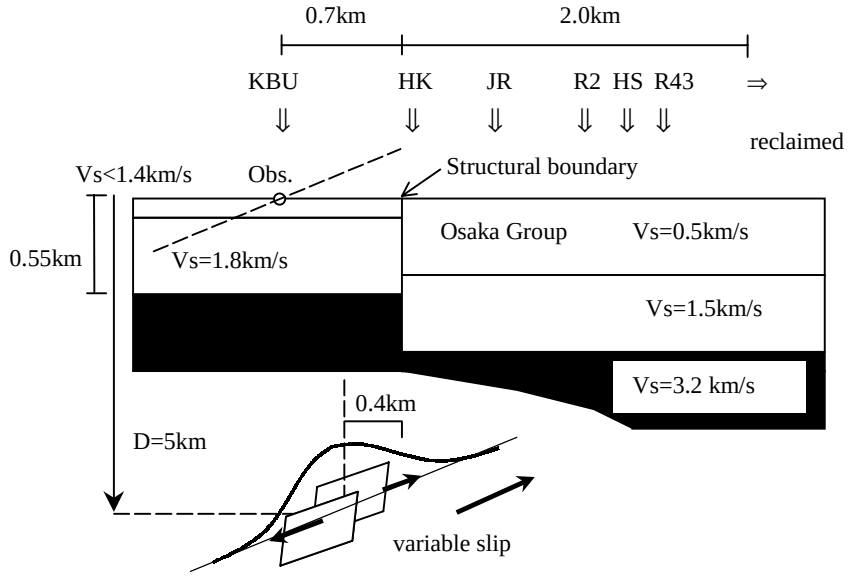

Figure 1: Analyzed irregular underground structure for variable slip rupture source.

ANALYTICAL METHOD

Outline of method

3D wave propagation analyses have been performed using the 2D deep irregular underground structure model of Kobe City. The hyperelement method [Nagano and Motosaka, 1995] has been applied to the wave propagation analysis for a finite moving source with variable slip. As a source mechanism, the strike slip case of a vertical fault is investigated in this study (ref. to Fig.1). Instead of calculating the displacement wavefield due to the moving double couple with variable moment M in the positive y direction, the shear strain γ_{xy} wavefield is calculated for moving single force with amplitude of the moment M in the negative y direction based on Maxell-Betti's reciprocity theorem.

Basic equations and mathematical expressions of a finite moving body force

Equation of motion in 3D-elastic body is expressed as Navier's equation in the following form.

$$(\lambda+2\mu)\mathrm{graddiv}\mathbf{u}-\mu\mathrm{curl}\cdot\mathrm{curl}\mathbf{u}+\mathbf{f}=\rho\frac{\partial^2\mathbf{u}}{\partial t^2} \tag{1}$$

Wher λ and μ are Lame's constants. ρ is mass density. The vectors **u** and **f** denotes the displacement and the body force, respectively. A moving source with constant velocity c at $z = z_s$ is considered on y-z plane. A finite variable moving body force **f** is expressed in the following form using unit vector $\mathbf{e}_i$ in i direction.

$$\mathbf{f}=\mathbf{e}_i P_i(x,y,z,t) \tag{2}$$

$$P_i(x,y,z,t)=\overline{A}_i(y)\delta(x)\delta(y-ct)\delta(z-z_s)\otimes g(t)$$

$$\overline{A}_i(y)=\frac{A_0}{2}+\sum_{i=1}^{N/2-1}\left[A_k\cos\left(\frac{2\pi k}{N\Delta L}y\right)+B_k\sin\left(\frac{2\pi k}{N\Delta L}y\right)\right]+\frac{A_{N/2}}{2}\cos\left(\frac{\pi}{\Delta L}y\right)$$

In the above equation the variable $\overline{A}_i(y)$ is expressed as the discrete Fourier transform. The symbol $\otimes$ denotes convolution integral. Applying Fourier transform to eq.(2), the moving body force in the frequency-wave number (F-K) domain is expressed as the following form [Nagano and Motosaka, 1995].

$$\tilde{\tilde{P}}(k_x, k_y, z, \omega) = 2\pi\delta(z - z_s)\cdot[C_0\delta(k_y - \frac{\omega}{c}) + \sum_{k=1}^{N/2-1}\{C_k\delta(k_y - \frac{\omega-\omega_k}{c}) + C_k^*\delta(k_y - \frac{\omega+\omega_k}{c})\} + \frac{C_{N/2}}{2}\{\delta(k_y - \frac{\omega-\omega_{N/2}}{c}) + \delta(k_y - \frac{\omega+\omega_{N/2}}{c})\}]\cdot G(\omega) \quad (3)$$

where

$$C_k = \frac{A_k - iB_k}{2},\ C_k^* = \text{conjg}(C_k) \text{ and } \omega_k = \frac{2\pi ck}{N\Delta L}$$

As described in above equation, the variable moving body force in the F-K domain is expressed as summation of *N* wave number components. The center wave number is ω/c and wave number discretization is $2\pi / N\Delta L$.

Numerical model and analytical conditions

The analyzed geological structure is the graben-like underground structure corresponding to the north-south section through Kobe University as shown in Fig.1 [Motosaka and Nagano, 1997]. The soil profiles at rock and sediment sites are tabulated in Table-1 and 2, respectively. Line sources with different slip distributions are considered. Depth of the source is assumed to be 5km at x-coordinate of –0.4km. One and two asperities cases are considered as shown in Fig.2. For the one asperity case (Fig.2(a)), two different asperity sizes are investigated. Each slip distribution is assumed to be Gausssian distribution. Two different parameters are adopted, *l*=5 and 10km as shown in Fig.2. Note that the standard deviation (σ) to determine Gaussian distribution is 1.25km for *l*=5km and 2.5km for *l*=10km. For 1-asperity cases, the slip displacements are determined such that the total seismic moment becomes the same in the two cases. Unilateral rupture propagation is assumed. Rupture velocity is assumed to be 2.5 km/s. Rate of the used source time function is indicated in Fig.3. The rise time is assumed to be 1s and the maximum velocity (v_{max}) is determined such that the slip displacement becomes the value corresponding to the slip distribution at each point. Center of the slip distributions is assumed to be y=0. For the 2-asperities cases (Fig.2(b)), the two asperity sizes are assumed to be the same, namely $d_2=d_1$ and *l*=5km. Two different distances between the asperities are investigated, namely R_a=25km and R_a=10km. Note that the location of the second asperity is the same y=0 in the two cases.

Table 1: Soil profile at rock site.

Layer No.	*Vs (m/s)*	*Vp (m/s)*	*γ (t/m³)*	*Thickness (m)*
1	850	2050	2.1	12.2
2	960	2250	2.1	7.45
3	1120	2850	2.1	12.5
4	1350	3100	2.2	67.85
5	1800	5500	2.4	450.0
6	3200	5700	2.5	∞

Table 2: Soil profile at sediment site

Layer No.	*Vs (m/s)*	*Vp (m/s)*	*γ (t/m³)*	*Thickness (m)*
1	500	2200	2.1	450.0
2	1500	2800	2.2	400.0
3	3200	5700	2.5	∞

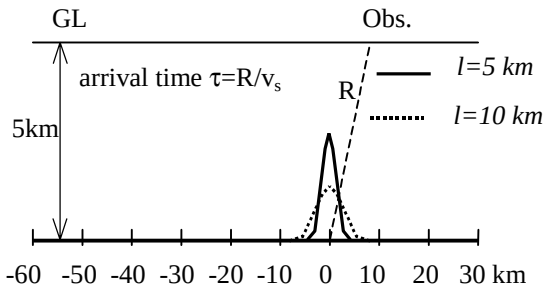

(a) one asperity

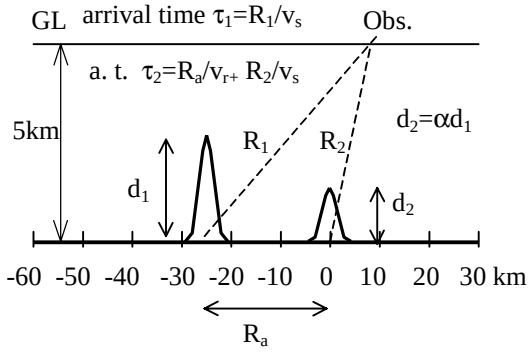

(b) two asperities

Figure 2: Used slip distributions.

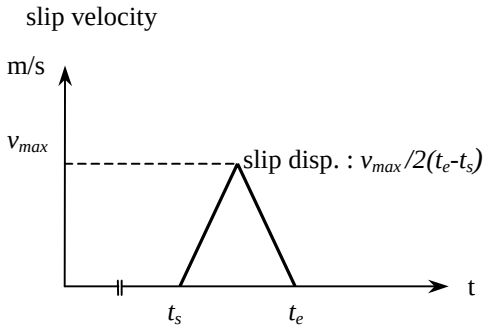

Figure 3: Rate of source time function.

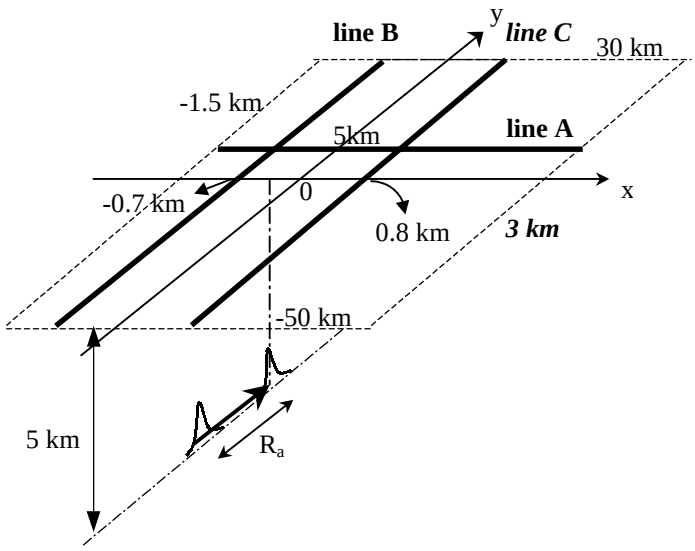

Figure 4: Calculation area.

Ground motions are calculated in the bounded region by dotted lines indicated in Fig.4 and the contour figures of the Peak Ground Velocities (PGVs) are investigated. The velocity waveforms are calculated along the three lines indicated in this figure. Along line-A, perpendicular to the structural boundary, the velocity waveforms are calculated at 46 equally spaced points with 100m separation. Along line-B and line-C, the waveforms are calculated at equally spaced points with 2.5km separation. It is noted that line-B at rock site, parallel to the structural boundary, corresponding to the location of Kobe University (x = -0.7km). Line-C at sediment site, parallel to the structural boundary, corresponding to the center of the heavily damaged belt zone (x=0.8km), where the calculated ground motion becomes the largest [Motosaka and Nagano, 1997] for the plane incident waves, deconvoluted from the observation records at Kobe University.

The widely used frequency response analysis was performed using FFT algorithm to calculate the waveforms. Discretization in the y direction is selected as ΔL=1.25km. The number of discretization is assumed to be N=190. The periodic length of discrete Fourier transform is L=237.5km. The analyzed frequency is 0-3 Hz. The discretization in frequency is selected as Δf=1/4096s.

ANALYTICAL RESULTS

1-asperity cases

Fig.5 shows velocity waveforms in the FN, FP and UD directions along line-A for l=5km. It is found that the ground motions in the FN direction have larger amplitudes than the FP direction and the ground motions in the FN direction at the sediment site are nearly amplified by 3 times from those at the rock site. The location where the PGV shows the maximum value is 0.9 km from the structural boundary. The amplification seems to be due to constructive interference of the vertically propagating waves and the diffracted waves at the structural boundary. The contour figures of the PGV distributions are shown in Fig.6(a) and (b) for l=5km and l=10km, respectively. Note in Fig.6 that the distance in the x-direction is enlarged by ten times compared to the y-direction. The waveforms are calculated for unit seismic moment ($1.0\ t^f m = 9.8\text{x}10^3$ Nm $= 9.8\text{x}10^{10}\,\text{dyne}\cdot\text{cm}$). It is recognized that the PGVs for l=5km are larger compared to those for l=10km. It is confirmed that the ground motions in the FN direction are the largest. It is found that PGVs become large in the same range of x=0.7km~1.0km for both asperity sizes, where the calculated ground motion becomes large also for the plane incident waves, deconvoluted from the observation records at Kobe University [Motosaka and Nagano, 1997]. It is also found that the FN/FP ratio, the ratio of PGV in the FN direction to the FP direction, becomes larger as slip size becomes smaller. The vertical PGVs become large at the sediment site in the vicinity of the rock-sediment boundary. This result is the same as the plane wave incident case [Motosaka and Nagano, 1997].

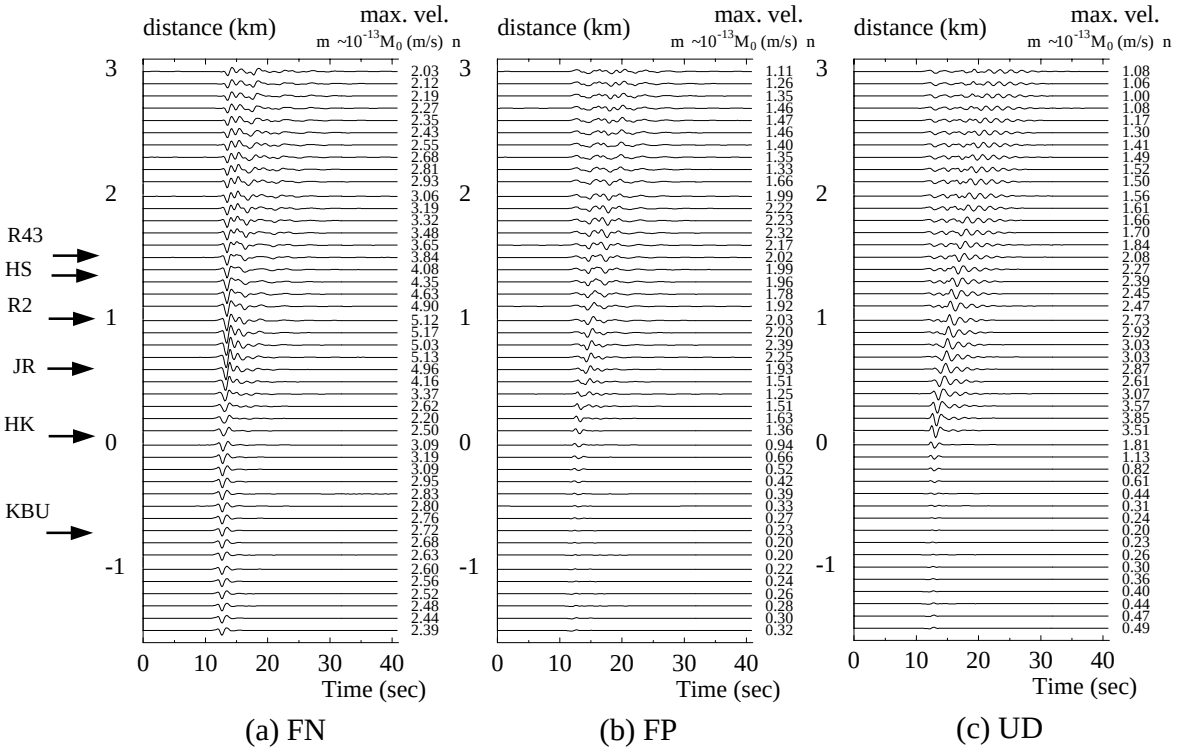

Figure 5: Velocity waveforms along line-A (*l*=5 km).

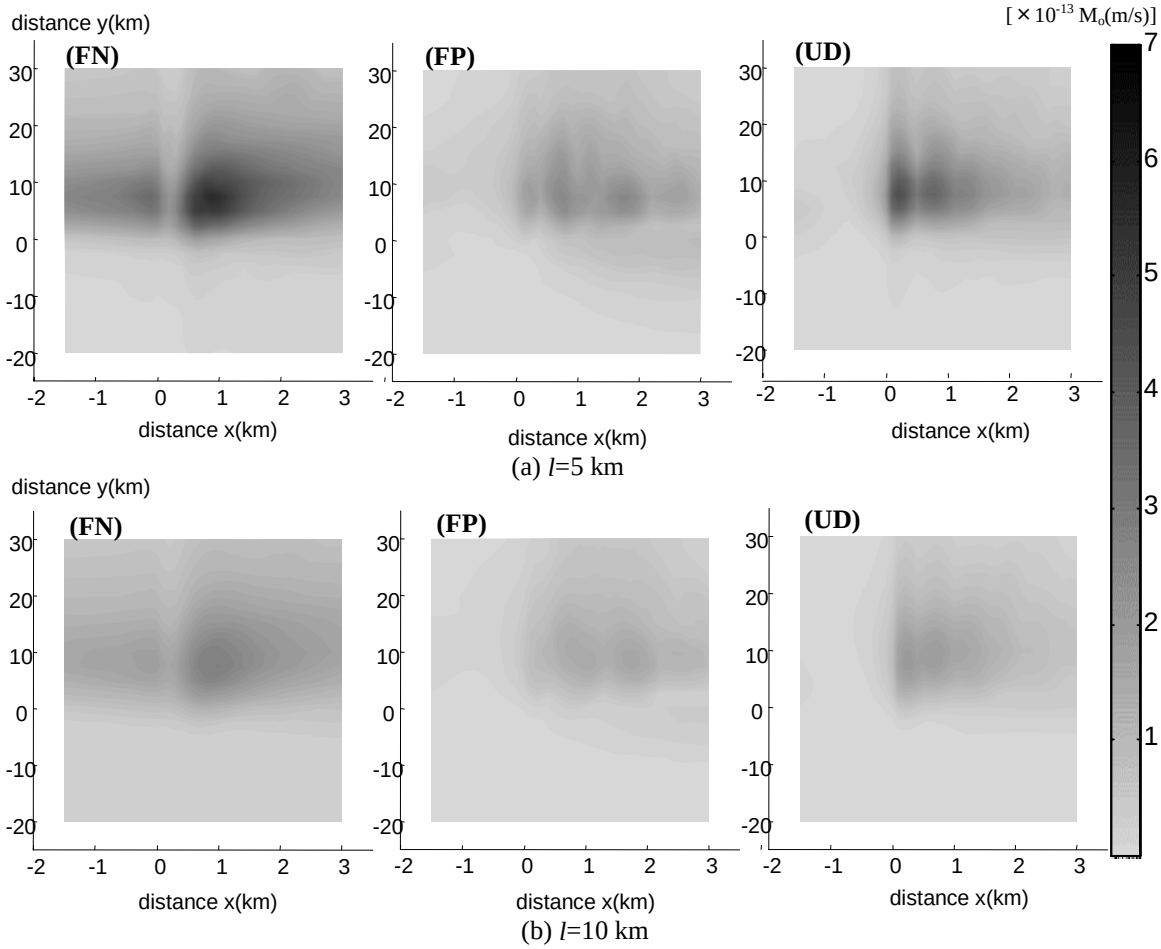

Figure 6: PGV distributions on ground surface.

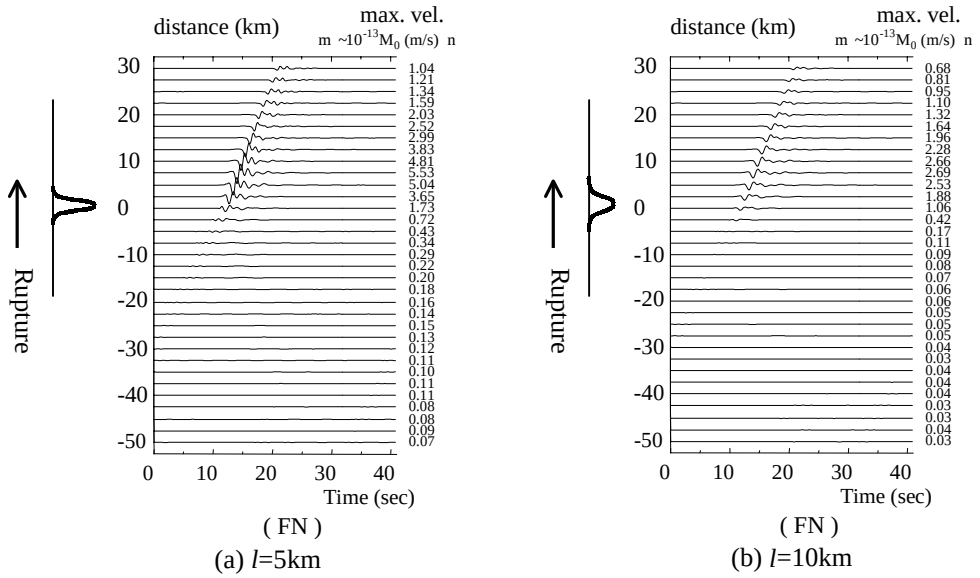

Figure 7: Velocity waveforms along line-C in FN direction (1-asperity case).

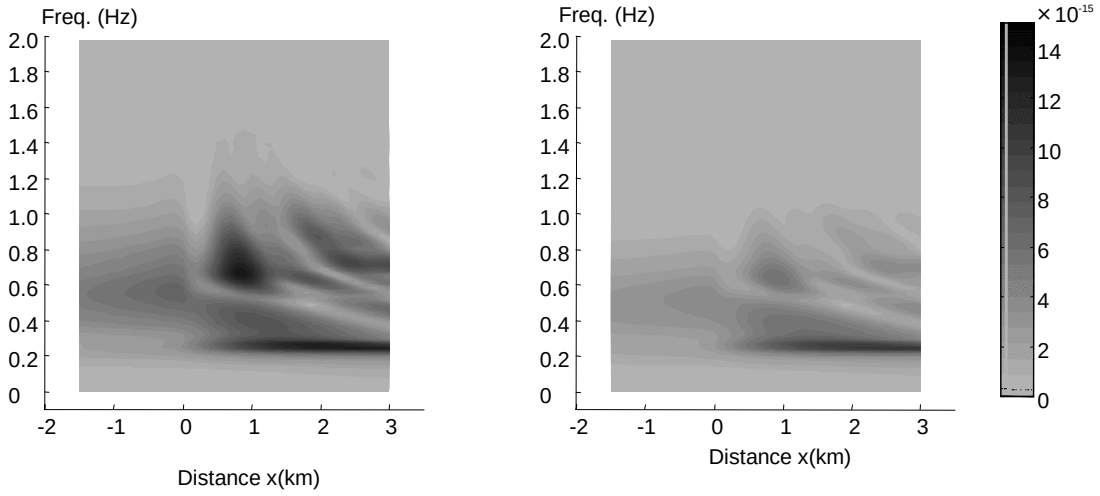

Figure 8: Fourier spectra of ground motion along line-A.

The velocity waveforms in the FN direction along line-C are shown in Fig. 7(a) and (b) for l=5km and l=10km, respectively. It is found from these figures that the strong directivity is recognized in the rupture propagation direction and that the location indicating the maximum amplitude is in the vicinity of the location where the rupture stops for both asperity sizes.

Fourier amplitude spectra of the ground motions in the FN direction along line-A are shown in Fig.8(a) and (b) for l=5km and l=10km, respectively. It is found that the higher frequency contents are included at rock site for the case of l=5km compared to the case of l=10km and at the sediment site the higher resonant frequencies are stimulated, as the slip size becomes smaller. It is also recognized that the dominant frequencies at sediment site are different in location. As the distance increases from the structural boundary, the higher dominant frequencies seem to become lower. This may be due to the effect of the dispersive waves generated at the structural boundary.

2-asperities cases

Fig.9 shows the velocity waveforms in the FN direction for the case of R_a=25km along line-B at rock site (a) and line-C at sediment site (b). Note that the y-coordinate of the first asperity is y=-25km and that of the second

asperity is y=0. It is recognized that the location where the contributions of the two asperities become the same, is just above the second asperity (y=0km), not the middle point of the two asperities (y=-12.5km). It is confirmed that the s-wave arrival time from each asperity coincides with the expected time shown in the legend of Fig.2.

In Fig.10, the PGV distributions in the FN direction are comparatively shown for the cases of R_a=25km and R_a=10km. Note that, for R_a=10km, the y-coordinate of the first asperity is y=-10km and that of the second asperity is y=0km. For R_a=25km, the ground motion distribution in the FN direction is almost the same as the corresponding 1-asperity case (ref. to Fig.6(a)). Namely, in this case the wavefields from the two asperities are almost independent. For R_a=10km , the wavefields from the two asperities are interfered each other and the ground motion distribution becomes quite different from the 1-asperity case.

Fig.11 shows the PGV distributions along line-C (corresponding to x=0.8km) in the FN direction for two cases. It is recognized that the maximum PGVs become smaller in this x-coordinate for R_a=10km compared to those for R_a=25km. But it is found from Fig. 10 that the PGVs become larger at some parts, e.g. in the x-coordinate of 2-2.5km.

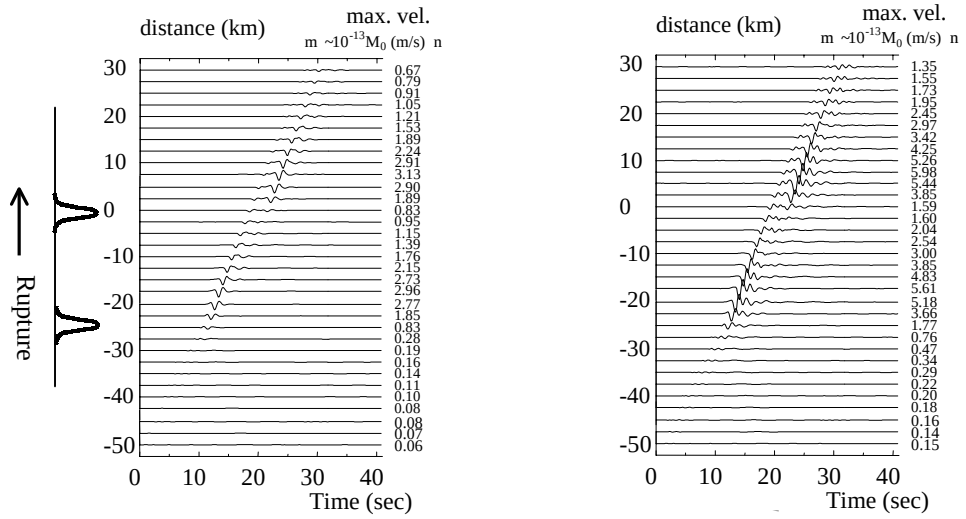

Figure 9: Velocity waveforms for 2-asperities case in the FN direction. (R_a=25 km)

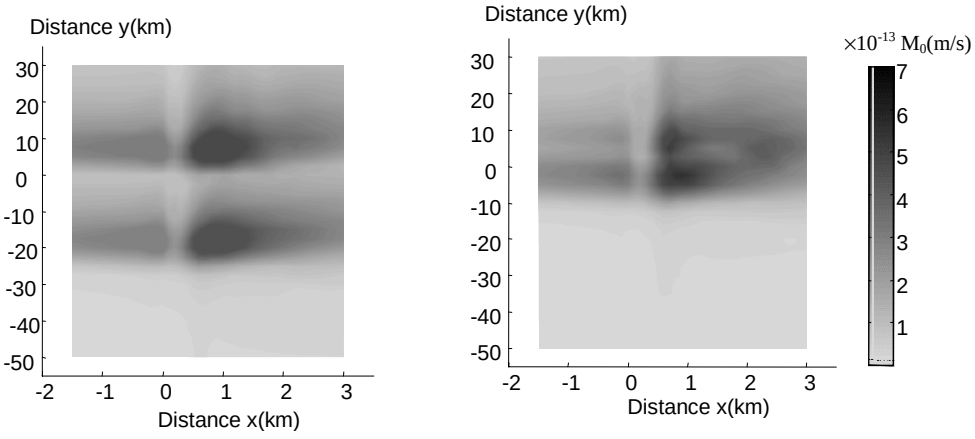

Figure 10: PGV distribution on ground surface in the FN direction for 2-asperities cases.

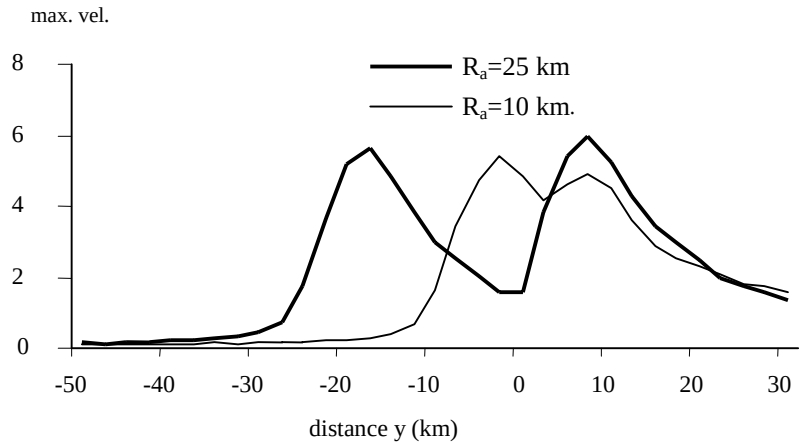

Figure 11: PGV distributions along line-C in the FN direction for 2-asperities case.

CONCLUSIONS

Ground motion characteristics taking into account the variable slip source and the graben-like underground structure model of Kobe City are analytically investigated using hyperelement method. Ground motion amplification characteristics at the sediment site to the rock site are discussed for one-asperity models with different sizes and also for two asperities models. Findings are as follows:

1) The amplitudes of the calculated ground motions in the FN direction are larger than the FP direction as recognized in the observed near-source ground motions. The FN/FP ratio, the ratio of PGV in the FN direction to the FP direction, becomes larger as slip size becomes smaller.

2) The PGVs in the FN direction become large in the same range corresponding to the heavily damaged area. The vertical PGVs become large at the sediment site in the vicinity of the rock-sediment boundary. These results are the same as those for plane incident waves, deconvoluted from the observation records at Kobe University.

3) The PGVs are larger in the smaller asperity case compared to the larger asperity case when the total seismic moments are the same. The higher frequency contents are generated at the rock site and e the higher resonant frequencies are stimulated at the sediment sit as the slip size becomes smaller.

4) It is confirmed that the calculated waveforms show strong forward directivity in the propagation direction due to a finite moving source and that the shape of the PGV distribution for one asperity can be changed due to the interference of the wavefields for two asperities when they are closed.

REFERENCES

Motosaka, M. & M. Nagano (1997). "Analysis of ground motion amplification characteristics in the heavily damaged belt zone during the 1995 Hyogo-ken Nanbu Earthquake", *Earthquake Engineering and Structural Dynamics*, 26: 377-393.

Motosaka, M. & H. Takenaka (1998). "Theoretical ground motion characteristics considering variable slip source and irregular underground structure", *Proc. of 2nd int'l symposium on the effects of surface geology on seismic motion*, Vol.2, 1075-80

Nagano, M. & M. Motosaka (1995). "2D response analysis of structure for plane waves with arbitrary incident angle", *Journal of Structural and Construction Engineering, Trans. of AIJ*, 474: 67-76.